Title: Influence of collars on the primary stability of cementless femoral stems: A finite element study using a diverse patient cohort

Rami M A Al-Dirini*

Email: rami.aldirini@flinders.edu.au

Medical Device Research Institute (MDRI), School of Computer Science, Engineering and Mathematics, Flinders University, 1284 South Road, Clovelly Park, Adelaide, Australia 5043

Daniel Huff,

Email: dhuff4@its.jnj.com

DePuy Synthes,

Johnson and Johnson

Warsaw, USA

Ju Zhang,

Email: ju.zhang@auckland.ac.nz

Auckland Bioengineering Institute,

Auckland University

Auckland, New Zealand

Thor Besier,

Email: t.besier@auckland.ac.nz

Auckland Bioengineering Institute & Department of Engineering Science,

Auckland University

Auckland, New Zealand

John G Clement,

Email: johngc@unimelb.edu.au

Melbourne Dental School, University of Melbourne

Melbourne, Australia

Mark Taylor

Email: mark.taylor@flinders.edu.au

Medical Device Research Institute (MDRI), School of Computer Science, Engineering and Mathematics Flinders University

Adelaide, Australia 5043

Running title: Influence of collars on the primary stability of THR

Abstract (word count: 357 words)

For cementless femoral stems, there is debate as to whether a collar enhances primary stability and load transfer compared to collarless designs. Finite Element (FE) analysis has the potential to make comparisons of stem designs within the same cohort of femora, allowing for subtle performance differences to be identified, if present. Subject-specific FE models of intact and implanted femora were run for a diverse patient cohort (41 femora, 21 males; BMI 16.4 – 39.8 kg.m^{-2}, 20 females; BMI 18.7 – 41.2 kg.m^{-2}) of joint replacement age (50 - 80 yrs). Collared and collarless versions of Corail® (DePuy Synthes) were sized and positioned using an automated algorithm that aligns the femoral and stem axes, preserves the head centre location and achieves maximum metaphyseal fit, while respecting the cortical bone boundaries. Joint contact and muscle forces were applied simulating the peak forces associated with level gait and stair climbing and were scaled to the body mass of each subject. A holistic approach was used to assess three failure scenarios: the potential for formation of peri-prosthetic fibrous tissue (bone-stem micromotion), the potential for peri-prosthetic bone damage (interfacial equivalent strains) and bone remodelling (rate of change in strain energy density, per unit mass) of collared and collarless designs, with focus on the calcar region of the bone. Comparisons across a range of performance metrics was assessed using paired t-tests. Only subtle differences were found as similar micromotion (mean of 90th %ile for collared = 86 µm and for collarless = 92.5 µm), interface strains (mean of 90th %ile for collared = 733 µε, mean for collarless = 767 µε) and bone remodeling stimuli were predicted for collared and collarless designs. As a result, the addition of a collar is unlikely to cause major differences in the biomechanics of bone-implant interaction. The slight differences observed are likely to be superseded by those induced by patient characteristics. ***Statement of Clinical Significance***: Our results suggest that the presence or absence of a collar does not substantially alter the initial mechanical environment and hence is likely to have minimal clinical impact. Further analysis using different femoral stem designs is recommended before generalising these findings to other stems.

Key words: population FEM, cementless femoral stem, patient variability, total hip replacement, primary stability.

Word Count: 5,174 words

Introduction

The success of cementless femoral stems is dependent on achieving primary stability, which allows bone ongrowth and successful osseointegration [1-3]. Geometric design of a stem contributes to the primary stability and the load transfer from the stem to the bone [4, 5]. To improve the load transfer to the medial calcar, several stems have been designed with a collar. The range of currently available femoral stems includes collarless stems (e.g. Accolade, Stryker), collared stems (e.g. Furlong, JRI Orthopaedics) or stems with options for both designs (e.g Corail, DePuy).

Collared stems have existed since the 1970s, yet the contribution of the collar to the primary stability of the femoral stem remains unclear. The potential benefits of a collar include the prevention of migration in the early post-operative period and improved load transfer to the calcar [6]. In contrast, it has been argued that a collar may limit the degree of press-fit achieved at surgery [7]. This may lead to a cantilever-like motion, and in cases where the stem subsides, the collar may impinge on the calcar causing bone resorption, which may eventually result in failure [6].

The choice between a collared and a collarless femoral stem appears to be largely based on surgeon preference [8]. For stem designs where both options exist, collarless stems appear to be used more, accounting for between 69% [9] and 76% [8] of all stems used. Nonetheless, national registries for joint replacements report between 12% [10] and 33% [11] of the most commonly used cementless stems in primary THA to be collared stems. Although there is conflicting evidence in the literature as to whether there is any benefit from the addition of a collar [12, 13], there have been few clinical or in vitro studies that have performed direct comparisons using the same stem design to remove confounding factors. Roentgen stereophotogrammetric analysis (RSA) has indicated that collarless stems have higher initial migration rates as compared to collared stems [14, 15]. However, once stabilized, collarless stems have similar, low migration rates as the collared version [14]. In single centre studies, no differences have been reported in hip scores, femoral radiolucencies and proximal femoral remodelling [16] or in the Sedel score (which provides information about radiographic appearance and function) [8]. Survivorship studies, based on the analysis of large patient cohorts within National Joint Registries have shown that there is no difference in mid-term survivorship [9]. In vitro studies have reported improved primary stability when using a collared stem [6, 13, 17, 18]. For example, Demey et al (2011) [6] reported that a collar increased the force required to initiate subsidence from 3129N to 6283N, however these forces are high in comparison to those experienced during activities of daily living (typical hip contact forces between 1500N and 2500N [19]).

Finite element (FE) modelling can provide detailed information of the initial mechanical environment, in terms of the interface strains and stem micromotion [20-23]. Prendergast et al (1990) [23] used an FE model to assess the effect of a collar on cemented stems. They concluded that a collar reduces the likelihood of bone resorption as they produced stresses closer to those of an intact femur, compared to collarless designs. Mandell et al (2004) [12] also used a simplified cylindrical models to investigate the effect of a range of collar options. They concluded that assumed benefits of a collared stem, compared to a collarless stem are greatly reduced when bony ingrowth was simulated [12]. Keaveny et al (1993) [22] used a single subject-specific FE model, developed from CT scans, to compare the influence of porous coating and collar support on the primary stability of cementless stems. They found that friction introduced by the porous coating had more influence than the collar on the overall stem stability, and that higher friction values resulted in more stable stems. Abdul-Kadir et al (2008) [24] also used a single femur model to compare the effect of a collar for a generic cementless stem. They reported that, compared to the collarless design, the collar prevented distal micromotion and reduced micromotion near the medial calcar. However, because the difference in micromotion between collared and collarless design was small, they concluded the collar adds little benefit to the primary stability.

Finite element analyses based on a single subject are unlikely to be representative of the entire THA population [25], yet, the majority of finite element studies have been performed on a single femur [22]. Population FE studies [26, 27], on the other hand, have the potential to compare different stem designs within the same cohort of femora for a range of different activities, allowing for subtle performance differences to be identified, if present. Despite this potential, most studies only consider level gait loads [28]. A single load case may be sufficient for patients with a sedentary life style, however, with the increased number of young and active patients undergoing THA surgeries, it is important to consider a broader range of forces that are representative of activities of daily living when assessing stem performance [29]. The purpose of this study was to investigate the effect of a collar on the primary stability of cementless femoral stems across a diverse cohort of femora based on two of the most commonly encountered daily activities; level gait and stair climb activities.

Methods

Sample selection

Post mortem CT scans of femora for subjects between 50 and 80 years old from the Melbourne Femur Collection (MFC) were used as a database representing total hip replacement (THR) patient population [30]. The database contained 189 femora from 189 individuals, consisting of 102 women and 87 men. All scans were obtained with an Aquilion 16 MDCT scanner (Toshiba Medical Systems Corporation, Tokyo, Japan) through a helical scan protocol and typical settings for clinical examination (tube current: 180 mA, 120 kVp). The slice thickness was 2.0 mm and the spacing was 1.6 mm. The in-plane pixel dimensions were 0.976 x 0.976 mm. Each scan also had a phantom (Mindways Software, Inc, Austin, USA), based on which densitometric calibration was performed.

The MFC was originally established with ethical oversight from the Victorian Institute of Forensic Medicine (ethics approval EC26/2000). Later radiological studies (which our current investigations are based upon) took place with VIFM approvals EC9/2007 and EC10/2007. Later, sole ethical oversight for the collection was transferred to The University of Melbourne ethics approval 115392.1. In addition, the protocol for this study was approved by the Southern Adelaide Clinical Human Research Ethics Committee (protocol number 420.13).

A statistical shape model [31] was used to segment the CT images, and extract external and internal surface geometries (.stl) for each femur in the database. In brief, this was achieved through iterative customisation of a generic piecewise-polynomial parametric mesh to represent the inner and outer cortical surfaces of the femoral surface as follows: (i) an active shape model was used to customise a generic mesh to approximate the femoral surface, (ii) cortical profile modelling was performed normal to the active shape mesh to estimate cortical thickness, and segment the inner and outer cortical surfaces, (iii) data from cortical profile modelling was used to further customize the active shape mesh to represent the inner and outer cortical surfaces. The generated surfaces were imported into ScanIP (Simpleware, Exeter) and aligned with the CT images to generate masks defining the external and internal boundaries of the cortical bone. A custom Matlab (version 2014b, Mathworks, USA) algorithm was used to obtain geometric measures describing the anatomy of each femur (Table 1 S-1). The study cohort was selected by searching for femora that represent the maxima, minima and medians for body mass, body mass index (BMI), age and stature as well as 14 anatomical parameters (Table 1 S-1). This reduced the number of simulations run while still capturing the extremes of variation within the original sample. As a result, a total of forty four femora (23 males and 21 females) were selected for this study.

Preprocessing

For the selected sample, separate surfaces were generated for the external cortical bone and the inner cortex of each femur using a statistical shape model [31]. For each femur, the generated surfaces were imported into ScanIP (Simpleware, Exeter) and superimposed onto the CT images as segmentation masks. Greyscale data, with Hounsfield units (HU) were sampled from the CT scans as per the recommendation of the calibration phantom manufacturer (Mindways Software, Inc, Austin, USA). HU values were then converted to Young's moduli (E) using an established relationship [32]:

$$\rho = 0.989\ \mathrm{HU} + 9.89 \times 10^{-4} \qquad (1)$$

$$E = 10 + 6850\ \rho^{1.49} \qquad (2)$$

Where *E* is the Young's modulus (in MPa), and ρ is the apparent density (in g/cm^3).

FE models of intact femora were generated by mapping the Young's moduli onto first order tetrahedral meshes of the intact femora, with element sizes with mesh size equal to or less than the voxel size of the CT scans. For each element in the mesh, HU values for the voxels bound within the element volume were averaged and assigned to the element. This procedure was performed for every element of the intact femur mesh, using ScanIP (Simpleware, Exeter). Peak joint contact and muscle forces associated with level gait and stair climbing were applied based on established, idealized load cases [33] and scaled to the body mass of the individual. The forces applied during level gait included the hip reaction force, the resultant of the abductors (gluteus maximus, medius and minimus) and the tensor fascia latae, and the resultant of the vastus lateralis muscle. A similar, simplified load case was used to simulate stair climbing, but with contributions of ilio-tibial tract and the vastus medialis muscles were also taken into account. The hip reaction force was equally distributed over the nodes within a diameter of 1 cm at the proximal surface of the femoral head. Muscle forces were also equally distributed over the nodes within a diameter of 1 cm from the insertions described by Heller et al. (2005) [33]. Femora were rigidly constrained at the condyles. All FE models were solved using the implicit FE solver in Abaqus 6.12 (Dassault Systèmes, France). The total deformation, equivalent strains and strain-energy density were recorded for each intact-femur model.

The statistical shape model used for segmentation has a root-mean-squared (RMS) accuracy of 0.9mm. Based on visual inspection, the statistical shape model generated reasonable estimates of the anatomy, but some deviation was noted for some subjects, mainly at the diaphysis. To ensure segmentation errors do not influence the FE estimates used to assess primary stability, intact femur models that predicted maximum total (bending) deformation greater than 1.5 times the interquartile range of the sample, or strains exceeding the yield point of bone (7000 $\mu\varepsilon$ [34]) in the proximal third of the femur under the simulated loads were identified and manually segmented. The previous steps were then repeated to generate FE models from manually segmented images.

Two sets of FE models for the implanted bone were generated; one with the collared and the other with the collarless version of the 135° standard offset Corail® stem (Top left corner of Figure 1). The generation of implanted femur models was automated using a custom Matlab (version 2014b, Mathworks, USA) pipeline (Figure 1), as follows: (i) solid CAD geometries were created for the intact femora using the surface meshes generated by the statistical shape model, (ii) appropriate stem size, position and orientation were selected for each femur and applied to the solid CAD geometries of the stem to align it within the solid femur model, (iii) resection plane and cavity preparation were performed using Boolean operations in Hypermesh (Altair Engineering, Troy, MI) assuming a perfect match between the stem and cavity and that, for the collared stem, the collar achieves full contact with the resected bone surface, (iv) based on the mesh convergence study (see S-4 for details) implanted geometries were then meshed to generate a linear tetrahedral mesh with element sizes between 0.5 mm and 0.8 mm (Figure 1 S-4), using Hypermesh (Altair Engineering, Troy, MI), (v) material properties were mapped from the intact femur models to the implanted femur models by (a) aligning the intact and the implanted models in 3D space (b) the average material properties of intact mesh elements within the volume of each element in the implanted mesh was calculated and assigned to that implanted element, (c) this was repeated for each element in the implanted mesh, (vi) level gait and stair climb loads applied to the intact models were mapped to the implanted models, (vii) line-to-line contact was implemented (i.e. with no interference fit) over the entire length of the stem, using a surface-to-surface contact with a coefficient of friction of 0.6 (Figure 2 S4) and allowing for small sliding [21], (viii) all models were solved using Abaqus 6.12 (Dassault Systèmes, France) , and custom Matlab (version 2014b, Mathworks, USA) codes were used to post-process the solved FE models.

To ensure consistency in the positioning and sizing, a collared version was initially sized and positioned into each femur using custom algorithm. The algorithm positioned each of the available sizes (8 through to 20, with 8 being the smallest size and 20 being the largest size) for the standard offset Corail® femoral stem by aligning the trunnion axis with the femoral neck axis, and the stem long axis with the femoral shaft axis, while minimising the vertical offset between the trunnion centre and the femoral head centre. For such a position, the algorithm calculated the “gap” between the inner boundary of the cortical bone and the outer surface of the stem, at six equally spaced cross-sections along the stem long axis. The stem sizes with negative gaps (indicating an overlap) were discarded, and the size with the smallest positive gaps in all cross-sections was selected. This ensured that the size selected achieved maximum fill of the medullary canal without breaching the cortical bone boundaries. Femoral geometries were then resected by a plane parallel to the collar plane of the sized and positioned stem.

Another set of models was generated with collarless instead of collared stems by applying the same position, alignment and size of the collared stems to the collarless stems. Again, linear tetrahedral meshes of the same density and element size were generated for the collarless models.

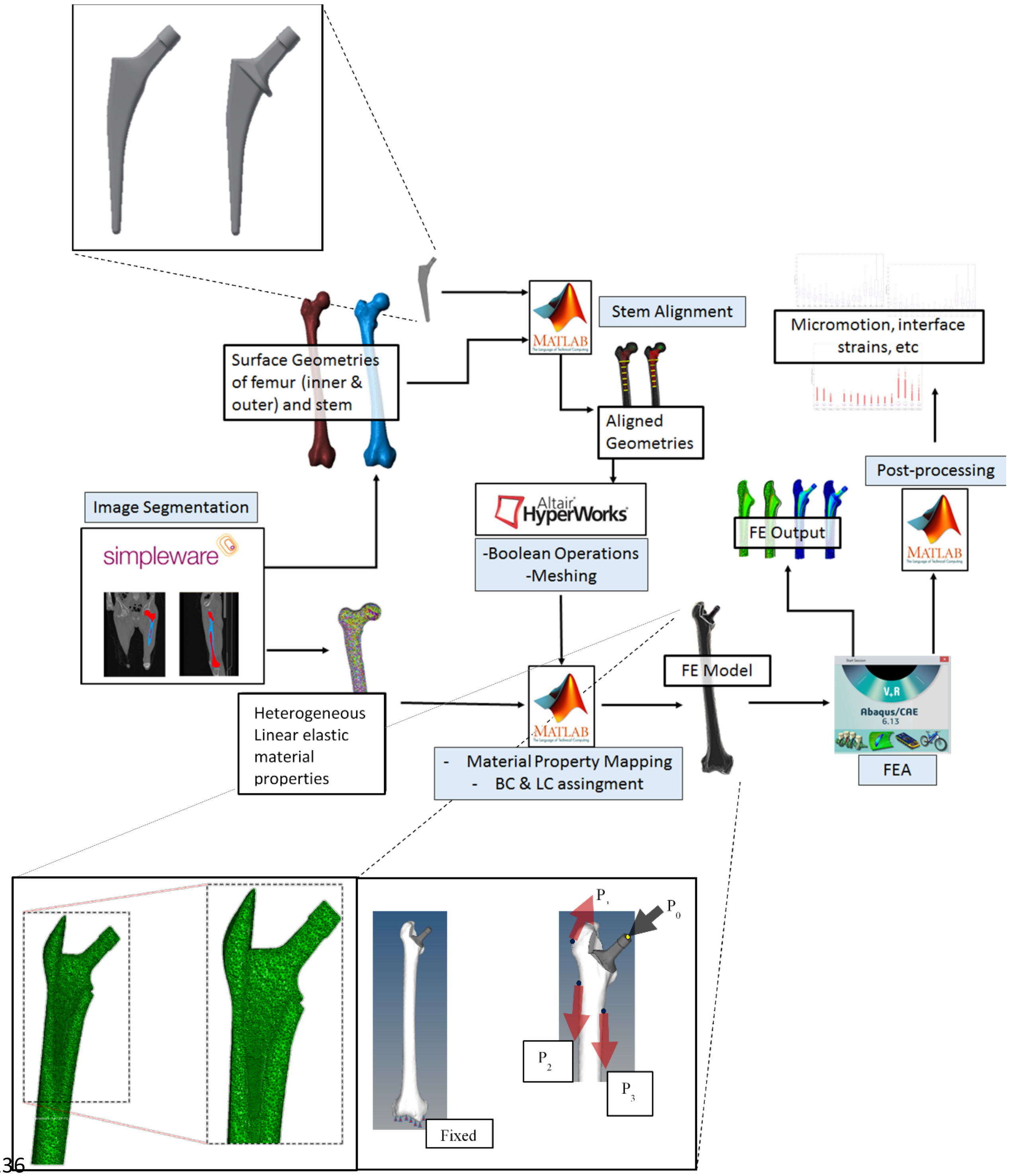

Figure 1: An automated pipeline was used to generate, solve and post-process subject-specific models. For each of the included subjects, CT scans were segmented using a statistical shape model. Material properties were assigned from Greyscale data and converted to Young's moduli. Collared and collarless versions of the standard offset Corail (top left corner) were sized and positioned into each subject so that boundaries of the internal anatomy are respected. Intact and implanted femur models were then meshed. Level gait was simulated by applying the joint reaction force through the head centre (or trunnion centre for implanted models) (P_0), the resultant of the abductors and the tensor fascia latae at P_1 and the resultant of the vastus lateralis at P_2. Stair climb simulations also included contributions of ilio-tibial tract and the vastus medialis muscles at P_3. For both activities, the distal nodes at the condyles were fixed.

Post-processing

A holistic approach was adopted to evaluate performance, based on the methodology developed by Martelli et al (2005) [20], to assess the risk of fibrous tissue formation, peri-prosthetic bone damage and bone resorption. The potential for fibrous tissue formation was assessed by examining the micromotion at the stem-bone interface. To calculate the micromotion of a stem, initial correspondence was established between the stem and the femur nodes prior to any deformation. For each stem-bone node pair, the total micromotion was defined as the difference in resultant displacement between the two nodes. The median and the 90th percentile micromotion were recorded for each femur. In addition, the percentage of the stem area experiencing micromotions less than 50 microns and greater than 150 microns were also recorded.

The potential for peri-prosthetic bone damage was assessed by examining the equivalent strain (Equation 3) at each of the elements at the stem-bone interface.

$$\varepsilon_{eq} = \frac{1}{\sqrt{2}} \left((\varepsilon_1 - \varepsilon_2)^2 + (\varepsilon_2 - \varepsilon_3)^2 + (\varepsilon_3 - \varepsilon_1)^2 \right)^{\frac{1}{2}} \quad (3)$$

Where ε_{eq} is the equivalent strain, ε_1, ε_2 and ε_3 are the first, second and third principal strains, respectively. The median and the 90th equivalent strains percentiles were recorded for each femur. The percentage area at the bone-stem interface experiencing strains > 7000 microstrains were also recorded for each femur [34].

Finally, the potential for bone resorption was assessed by examining the changes in strain-energy density (per unit mass). Changes in strain-energy density, per unit mass *(S)* were calculated by (i) mapping the strain-energy distribution, per unit mass, of the intact femur onto a point cloud, where the coordinates of each node were calculated by averaging the nodal coordinates for each element. (ii) In a similar fashion, the strain-energy density distribution, per unit mass, was mapped onto a point cloud of the implanted femur. (iii) Each of central nodes in the implanted femur model was paired to a central node in the intact femur model. For each node pair, the remodelling stimulus (s), measured by the change in strain energy density per unit mass (*S*) was calculated using Equation 4 for a region up to 8 mm away from the stem surface.

$$s = \frac{S_{implanted} - S_{intact}}{S_{intact}} \times 100\% \quad (4)$$

Where S_{intact} and $S_{implanted}$ are the strain energy density per unit mass for the intact and the implanted femora, respectively.

The percentage of the interface bone under high (s_{high}) and low (s_{low}) changes in strain energy density (per unit mass) were calculated as measures of bone remodelling stimuli. Thresholds for remodelling stimuli were defined as per Frost et al (1990) [35], with stimuli greater than 70% and less than -70% being assumed to promote bone apposition and resorption, respectively [1].

Paired t-tests were used to compare the two stem designs and unpaired t-tests were used to compare males and females. Linear regression was used to explore any significant correlation between patient characteristics (Table 1 S-1) and the median or the 90th percentiles micromotion and strain for collared and collarless stems (see Methods S-1 for details).

Results

Out of the 44 femora included in the study, three male and two female femora were manually segmented, as the automatically segmented intact femur models experienced excessive bending. Also, two male and one female femora were excluded due to failure in meshing the implanted geometry. Therefore, full analysis was performed on 41 femora (21 males and 20 females, see Table 1 S-1 for details).

At the cohort level, the predicted micromotion and interface strains were marginally higher and more variable when the collarless design was used, compared to the collared design, for both activities simulated (Figure 2 and 4). The micromotion and strains for both designs were also higher and more variable under stair climb loads compared to level gait loads, and on average, were also higher and more variable for males than females (Figures 2 - 5). Across the study cohort, the in micromotion were slightly more variable (140% relative to the median) than interfacial strains (120% relative to the median), particularly in the upper limit (90^{th} percentiles in Figures 2 and 4) of the micromotion and interface strains. However, the high variability (15% to 90%) was seen in the percentage area of the contact undergoing micromotion less than 50 microns (Figures 2 and 3). In contrast, the percentage area of the contact undergoing large > 7000 microstrains), or even small strains (<2000 microstrains) were somewhat consistent across the entire cohort (Figures 4 and 5).

Differences were found between collared and collarless design for the median micromotion and interface strain percentiles under level gait loads ($p < 0.05$) and stair climb activities ($p < 0.05$). In contrast, differences in the 90^{th} micromotion percentiles were only found for level gait activity. Differences were also found in the percentage area experiencing more than 7000 $\mu\varepsilon$ only for level gait activity ($p < 0.05$). No differences were found between collared and collarless stems' interface strains for both activities ($p > 0.05$) and no sex-based differences were found in the micromotion and interface strains ($p > 0.05$), for both designs under stair climb and level gait activities (Table 1 S3). Differences in bone remodeling stimuli (percentage change in strain energy density) were also found, but only around the medial calcar region ($p < 0.05$). Under level gait loads, the change in strain energy density in the calcar region ranged from 0% to 20% for the collarless design, and 0% to 10% for the collared designs. Similarly, under stair climb loads, the change in strain energy density in the calcar region ranged from 0% to 40% for the collarless design, and 0% to 30% for the collared designs. There were also no significant correlations found between any of the patient characteristics and the predicted micromotion or interfacial strains (Results S1). Trends were noted ($0.3 < r^2 < 0.6$) between interface strains and femoral anteversion angle, neck length, femur mass, and medial-lateral distance between the shaft axis and the head centre of the femur, however, only for stair climb loads (Table 2 S-1).

The micromotion predicted for most subjects with collared and collarless designs were mostly less than 50 µm. Small regions of the stem surface had elevated micromotion, sometimes exceeding 150 µm, however, for most subjects, these regions did not exceed 3% and 10% of the contact area during level gait and stair climb activities, respectively (Figure 2), and were localised around the resection surface and sometimes at the distal tip for both designs. Three subjects (1 male and 2 females) had greater areas which experienced high micromotions (>150 µm) during stair climb, with the collared design resulting in lower micromotion.

The strain pattern at the bone in contact with the stem was similar for the collared and the collarless designs. For both designs, relatively high strains (> 7000 με) were localised, for most subjects, at the distal tip of the stem. Relatively high interface strains were also observed at the lateral-posterior side near (or at) the resection surface, and the collarless design was noted to have slightly greater areas under high strains, compared to the collared design. An area at the lateral side at about mid-stem length was also noted to have high strains for both designs. However, these areas did not exceed 30% of the contact area for both designs during level gait and stair climb activities. Again, subjects that had relatively high micromotion had higher areas of interfacial strains (not exceeding than 30%) during stair climb (Figure 5).

Most of the bone volume more than 3 mm away from the stem surface experienced very small changes in the strain energy density ($-70\% < s < 70\%$), implying negligible no or little stress shielding. High bone remodelling stimuli (>>70%) was predicted for bone in direct contact with the stem, specifically at the anterior side near the resection surface from mid-stem to the distal tip of the stem. The high stimuli observed at the contact surface dissipated within 1 to 2 mm from the stem surface. No extensive resorption stimuli (< -70%) was recorded (Figure 6), indicative of no or little stress shielding.

On a subject-specific level, simulation results show that there was either no difference or a marginal improvement when a collar was used. Conversely, there were nine odd cases where a reduction in performance was noted when a collar is used (Figure 3 and 5). This was observed for all three performance metrics in this study (micromotion, interface strains and bone remodelling stimuli).

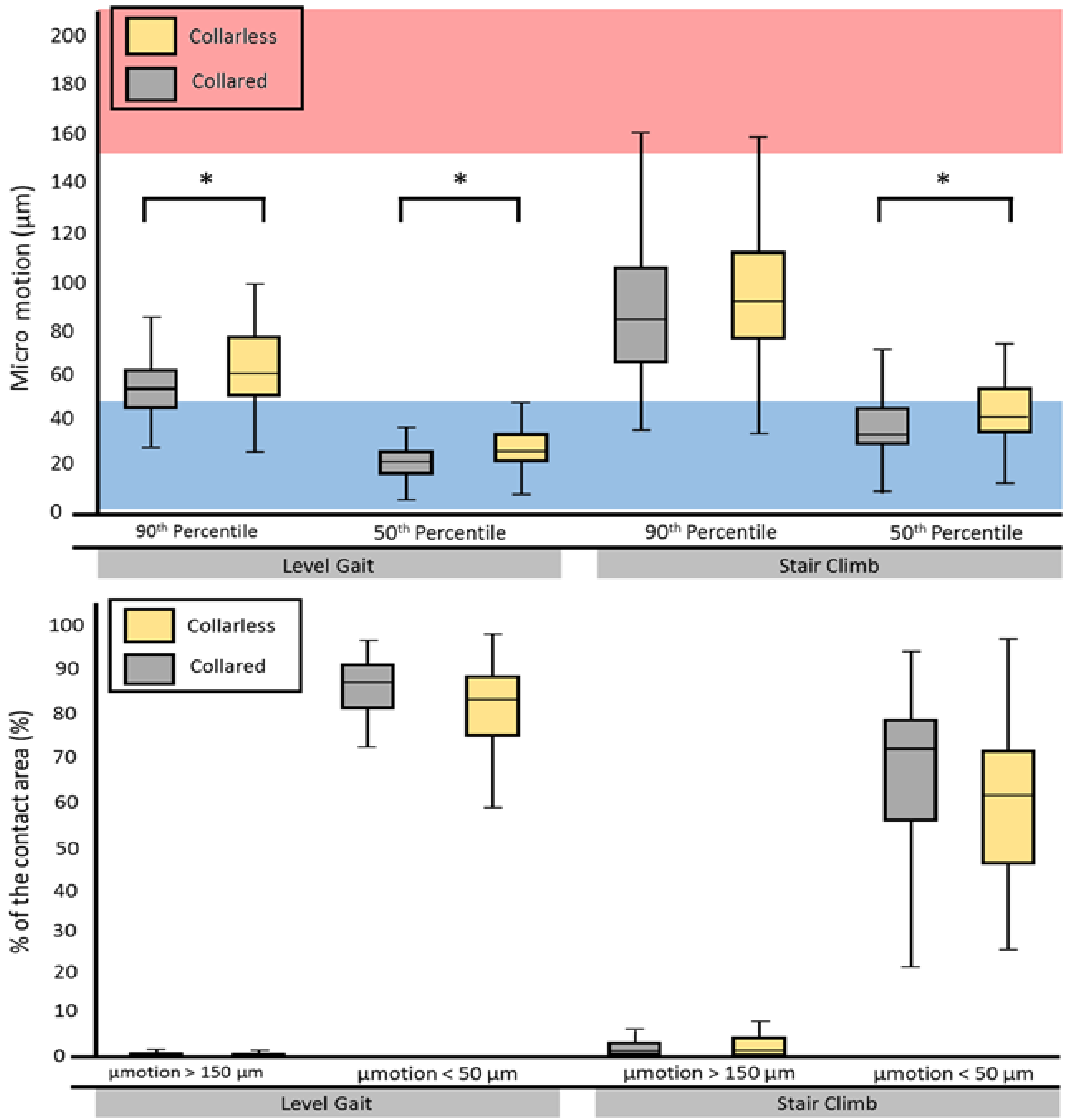

Figure 2: Micromotion profiles for collared (grey boxes) and collarless (yellow boxes) Corail® under level gait and stair climb activities across the study cohort. The top plot presents box plots for the predicted micromotion, in particular the 50th and the 90th percentiles, for level gait (left) and stair climb (right) activities. The red region indicates risk of fibrous tissue formation, which is undesirable for THA, whereas the blue region marks the threshold within which good bone osseointegration is expected. The bottom plot presents the ranges of the percentages of the contact area undergoing micromotion greater than 150μm and less than 50μm for level gait (left) and stair climb (right) activities. It can be seen that most of the stem-bone surface experienced micromotion below critical thresholds (50μm). Only a few subjects are expected to have less than 10% of the contact area under strains greater than 150μm. Statistically significant differences are shown with (*).

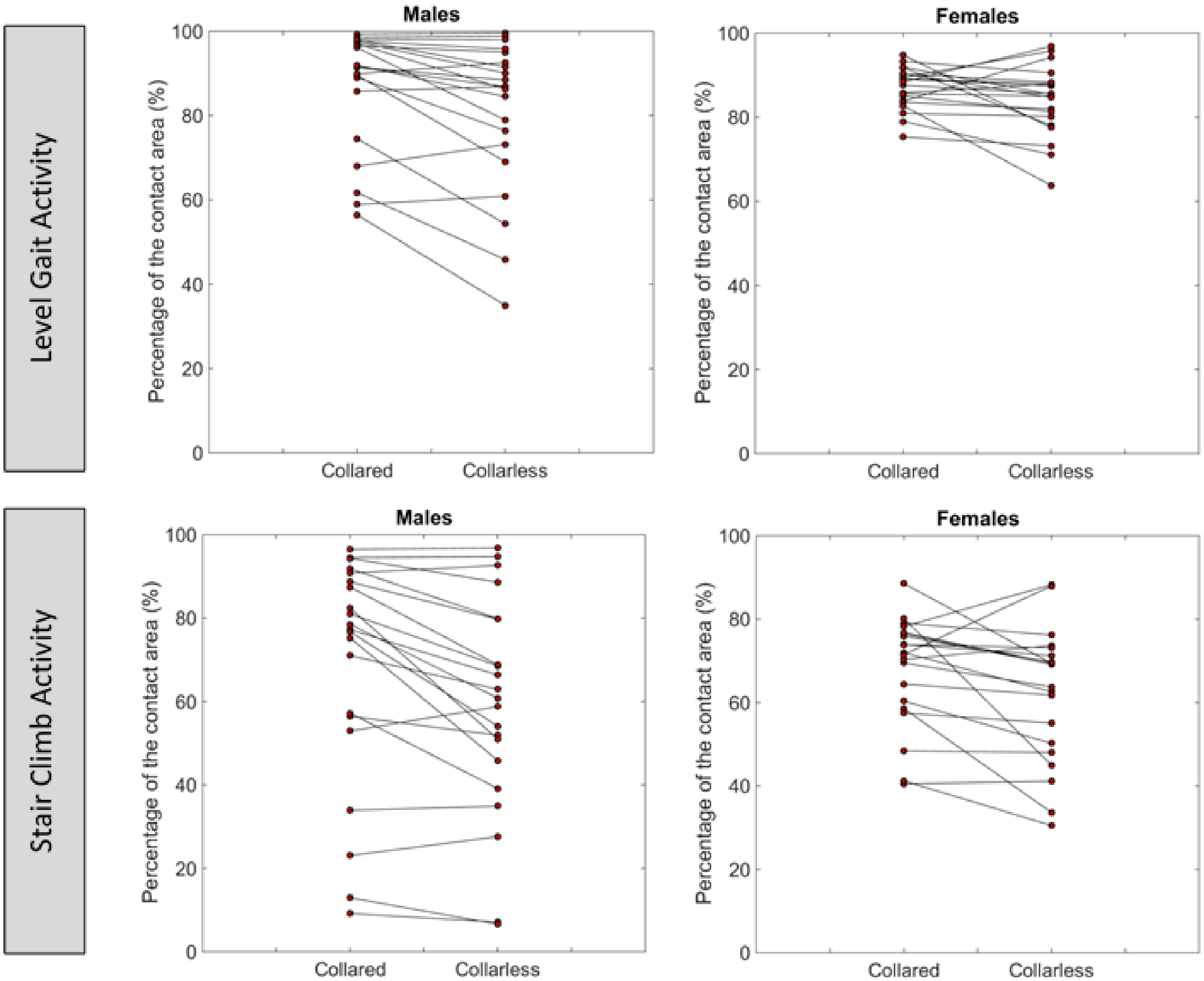

Figure 3: Percentage area of the bone-stem contact area experiencing micromotion less than 50 µm for level gait (top) and stair climb activities (bottom) for collared and collarless Corail®. The figure also presents predictions for males (left) and females (right) separately. It can be seen that stair climb loads resulted in greater variability and that males had more variability than females.

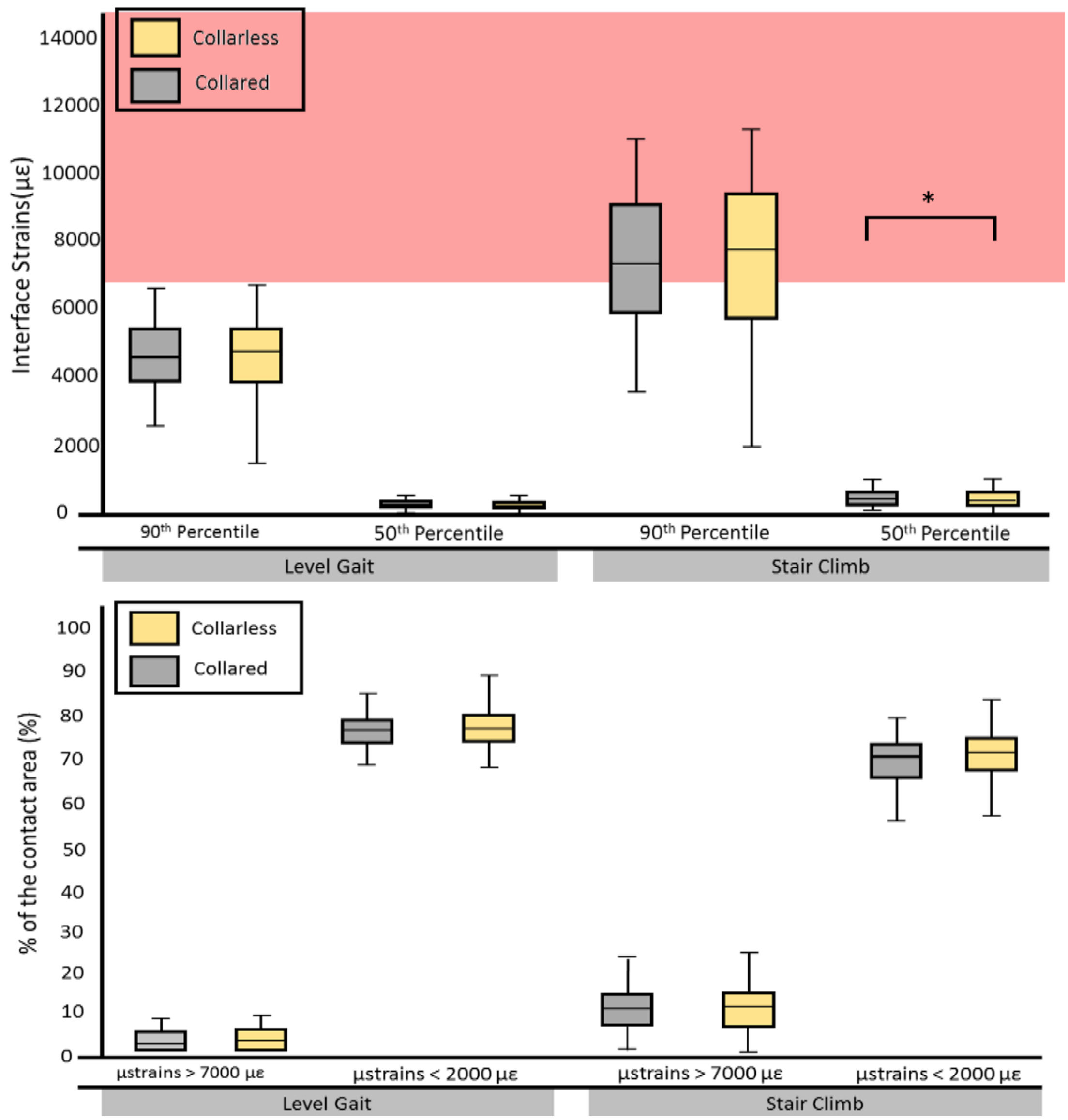

Figure 4: Interfacial strain profiles for collared (grey boxes) and collarless (yellow boxes) Corail® under level gait and stair climb activities across the study cohort. The top plot presents box plots for the predicted strains, in particular the 50^{th} and the 90^{th} percentiles, for level gait (left) and stair climb (right) activities. The red region marks bone yield threshold, which is undesirable in THA. The bottom plot presents the ranges of the percentages of the contact area experiencing strains greater than 7000 με and less than 2000 με for level gait (left) and stair climb (right) activities. The bottom plot shows that most of the stem-bone surface experienced strains below critical thresholds (7000 με). Only a few subjects are expected to have less than 30% of the contact area under strains greater than 7000 με. Statistically significant differences are shown with (*).

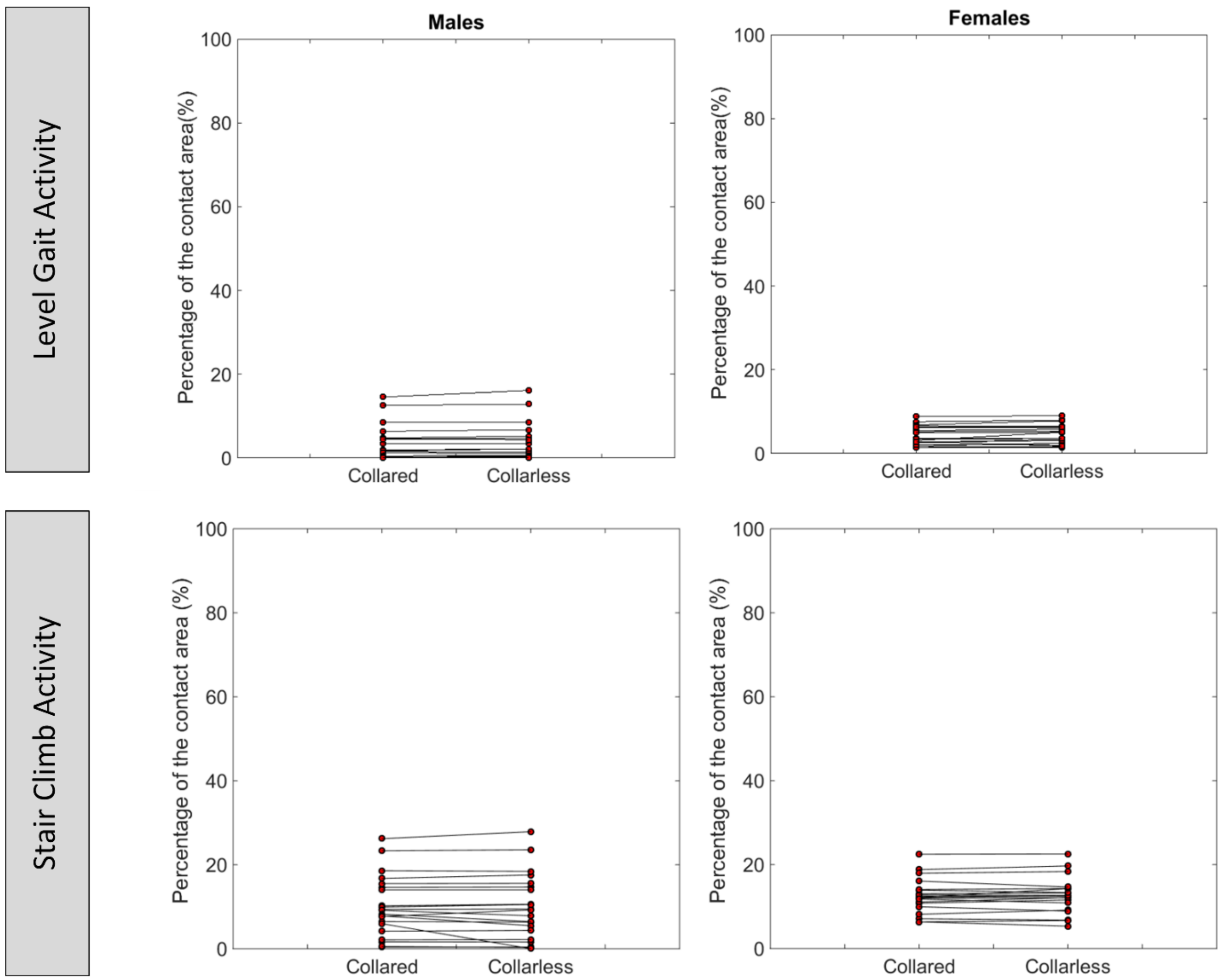

Figure 5: Percentage area of the bone-stem contact area experiencing interface strains greater than 7000 με for level gait (top) and stair climb activities (bottom) for collared and collarless Corail®. The figure presents males (left) and females (right) strains separately. It can be seen that stair climb loads result in greater variability in interface strains and that males had more variability than females.

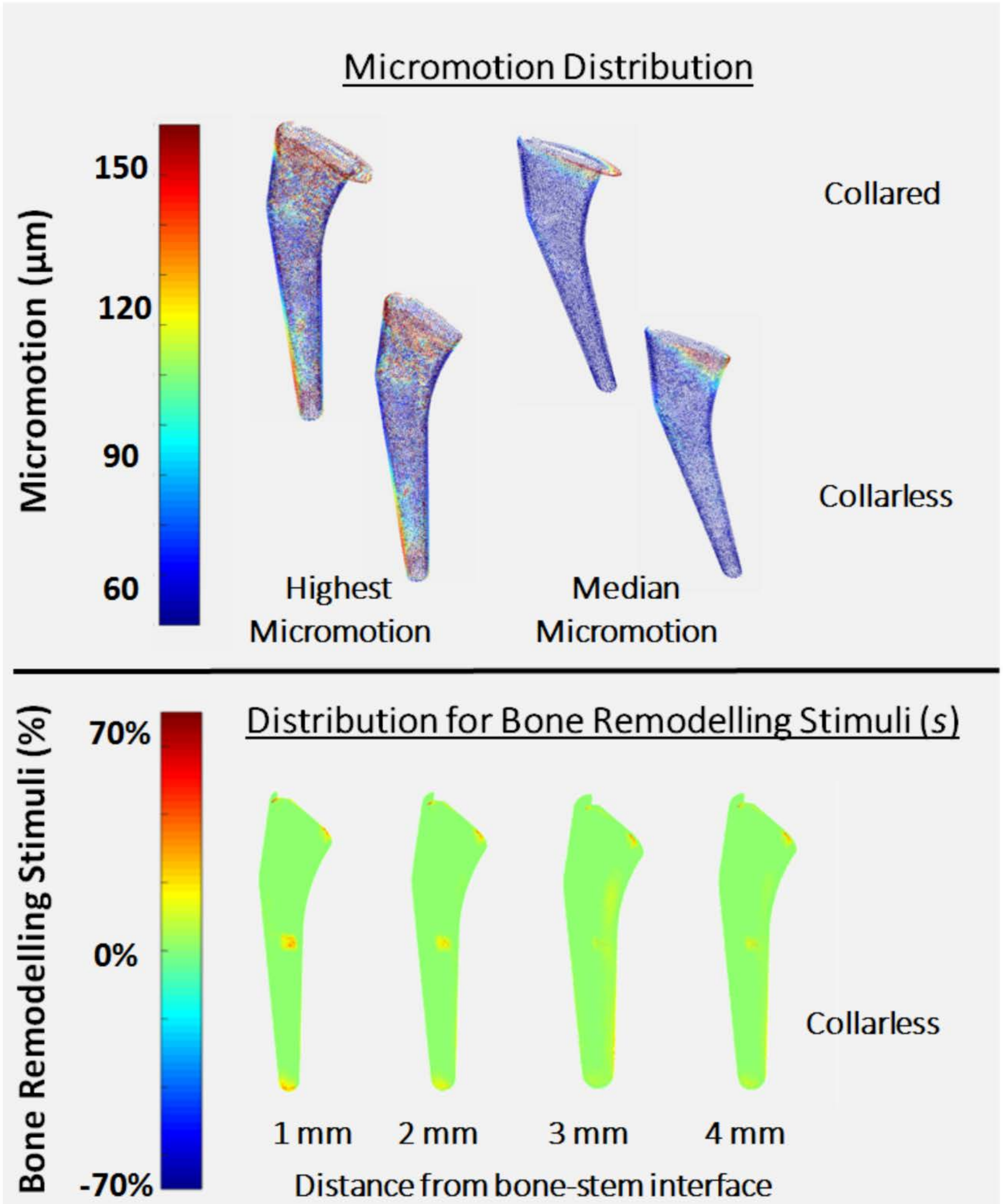

Figure 6: The top part of this figure shows the distribution of micromotion for two subjects during stair climb for collared and collarless stems, where the plots on the left show the distribution for the subject with the highest micromotion across the cohort, and the plots on the right show an average case. The bottom part of this figure shows the distribution of the bone remodelling stimuli (*s*), relative to the intact bone, under stair climb activity at various distances away from the bone-stem interface. The distances were (from left to right) 1mm, 2mm, 3mm and 4mm, respectively. Similar patterns were seen for the collared design, except for the high remodelling signal at the calcar region, which was absent when the collared design was used.

Discussion

In this study, load transfer and primary stability of collared and collarless femoral stems was compared for a diverse cohort of subjects (41 femora, 21 males; BMI 16.4 – 39.8 kg.m^{-2}, 20 females; BMI 18.7 – 41.2 kg.m^{-2}, see Table 1 S-1 for details) under level gait and stair climb loads using subject-specific FE modelling. The initial mechanical environment was assessed based on three main measures; micromotion, interface strains and changes in strain-energy density (per unit mass) relative to the intact femur of each subject. Only subtle differences were found between the collared and the collarless version of the stem, with the collared design having slightly less micromotion/strains than the collarless design, for most subjects. These differences are unlikely to have clinical impact, implying that a collar seems to have little influence on the load transfer and primary stability for the stem used (Corail®, DePuy).

Primary stability of femoral stems requires good osseointegration between the bone and the stem, which is likely to be achieved with micromotion below 50 μm [36]. In contrast, adverse changes such as fibrous tissue formation or peri-prosthetic bone damage is likely occur if the stem micromotion exceeds 150 μm [1] or if the strains at the bone-stem interface exceed 7000 με [34], respectively. Bone resorption may also occur in regions under low remodelling signal ($s < -70\%$) [35]. For both designs (collared and collarless), our FE predictions show that all three measures of primary stability fall within acceptable ranges, for most subjects.

Previous FE studies [22, 28, 37-39] on primary stability for cementless long femoral stems seem to focus on the micromotion as a measure of the primary stability, with other measures such as interfacial strains and changes in strain energy density getting less attention. In this study, we have adopted a holistic approach to evaluate the main mechanically driven failure modes. For all measures considered, the patterns and magnitudes predicted were similar to those reported in FE literature on cementless femoral stems [22, 28, 37-39]. In particular, the micromotion patterns were consistent with those reported for long stems by Keaveny et al (1993) [39] (peak of 356 μm) and even short stems by Bah et al (2015) [28] (Peak of 100 ± 7 μm and average of 7 ± 5 μm), yet, they were different to those reported for another long stem by Abdul-Kadir et al (2008) [24] (Peak of 20 μm). The differences noted compared to Abdul-Kadir et al (2008) are likely to be due to differences in the micromotion calculation algorithms, and/or differences in the boundary conditions assigned. Abdul-Kadir et al (2008) used an algorithm that updates the nodal correspondence in each step of the simulation [24], whereas we used the nodal correspondence established prior to deformation. Keaveny et al (1993) [39] used a similar algorithm micromotion algorithm, but did not model the collar explicitly. Instead, the collar-calcar contact was modelled by constraining nodes of the stem neck in all degrees of freedom, which is why no micromotion was predicted at the collar in their study [39], whereas our simulations show some sliding micromotion at the collar-calcar contact.

A much higher variability was seen in the percentage area of the contact undergoing micromotion less than 50 microns (Figures 2 and 3), compared to interface strains. While we have not extensively analysed our models to explain this observation, our hypothesis is that the percentage of the area undergoing small micrmotion is affected by the variation in morphology of the medullary canal, whereas the high strains are likely to be loca.lised around points where the stem is sitting very close to the cortical bone. As this behavior was noted for both designs, it is unlikely to affect our conclusions on the benefit of a collar. However, this is certainly an interesting observation that warrants further investigation in future research.

Several assumptions were made in this study. The models in this study aim to mimic the mechanical behaviour of femoral stems implanted in real femurs, however, the results were not validated by direct comparison against experimental measurements of micromotion nor interfacial strains. Femoral stems were positioned assuming ideal alignment between the stem and the femoral axes, and that full metaphyseal fill can be achieved, which may be difficult to consistently replicate in real surgeries. The simplified contact model used in this study does not account for boundary conditions that would be introduced by press fitting the stem into the bone, which is likely to increase the magnitude of the interface strains, but reduce the micromotion. In addition, variation in stem position is likely to affect the micromotion and interface strains [40, 41]. Hence, the absolute micromotion and interfacial strain values must be taken with care. For collared stems, complete calcar engagement was also assumed. This may be difficult to achieve in real surgeries. However, this is unlikely to affect the conclusions of this study, primarily because a collared stem that is not engaged with the medial calcar will effectively act as a collarless stem.

The strains predicted at the bone-stem interface were below the yield point of bone, for most subject during level gait. However, our simulations predicted between 5% and 30% of the bone-stem interface area is likely to experience strains in excess of 7000 $\mu\varepsilon$, during stair climbing. Several factors may have contributed to the elevated high strain values, including thickness of cortical bone, the generic and simplified muscle and joint reactions forces, etc. However, these elevated strains only affect a small region of the bone in contact with the stem (< 30% of the contact area). Considering that clinically stable stems have typically no more than 30% of their surface fully osseointegrated [42], these localised strains are unlikely to impact the primary stability of the implant, for most patients. Nonetheless, current FE models of implanted femurs lack validation for interfacial strain distribution [43], which means that the absolute strain values need to be taken with care.

This study also found that, for cases where differences between collared and collarless stems were observed, differences were magnified when stair climb loads were considered (Figure 2-5). This highlights the importance of considering more demanding tasks, such as stair climb when comparing the primary stability of different femoral stem designs for THR [29]. However, it must be noted that statistical analysis would require larger samples (N = 36) when stair climb loads are considered, compared to level gait loads (N =20) (see S-2 and Table 1 S-2 for details).

Previous clinical studies *"confirmed the absence of any significant influence"* of collars on femoral stem performance [8]. In this study only subtle differences were found, which are not expected to have clinical impact. This is because the overall performance of a femoral stem is dependent on several design parameters. Corail® is known to have good short and long term performance [44], so the presence of the collar may not influence performance. Further analysis using different femoral stem designs (preferably from different manufactures) is recommended before generalising these findings to other stems.

It was not possible to apply subject-specific muscle and joint reaction forces for the study cohort, as the CT data was collected from deceased subjects. Therefore, muscle and joint reaction forces were computed using an established generic musculoskeletal model [33] and scaled to the body mass of each subject. On a subject-specific level, this may introduce errors, but these errors are likely to dissipate when averaged over a cohort [45].

Conclusion

This study investigated the effect of a collar on the primary stability of femoral stems across a diverse cohort of femora. Although differences were found in micromotion and interface strains, these were small and considered to have minimal clinical impact, as they are likely to be superseded by differences induced by patient characteristics. This suggests that the use of collar is unlikely to cause major differences in the biomechanics of bone-implant interaction, enhance load transfer or improve the primary stability of a stem. Further analysis using different femoral stem designs (preferably from different manufactures) is recommended before generalising these findings to other stem designs.

Acknowledgment

This study was part of a project funded by an Australian Research Council (ARC) linkage grant, with partial funding from DePuy Synthes. Prof Taylor, Prof Besier and Prof Clement are chief investigators named on the ARC linkage grant. Dr Al-Dirini is employed on this project. Mr Huff is employed by DePuy Synthes.

The authors are grateful to the staff of the Mortuary and the Donor Tissue Bank at The Victorian Institute of Forensic Medicine Australia for their assistance in collecting the material upon which this study is based. The authors are also grateful to the families of the donors who gave permission for the collection of the material expressly for research.

Author Contributions Statement:

Dr Al-Dirini and Prof Taylor contributed to the study design, data analysis and interpretation, and drafted the manuscript. Prof Clement contributed in the data acquisition and critical revision of the manuscript. Dr Zhang and Prof Besier were involved in the data analysis and critical revision of the manuscript. Mr Huff was involved study design, data analysis and interpretation, and critical revision of the manuscript. All authors have read and approved the final submitted manuscript.

References

1. Pilliar, R.M., J.M. Lee, and C. Maniatopoulos, *Observations On the Effect of Movement On Bone Ingrowth Into Porous-Surfaced Implants.* Clinical Orthopaedics and Related Research, 1986. **208**: p. 108-113.
2. Soballe, K., et al., *Migration of hydroxyapatite coated femoral prostheses. A Roentgen Stereophotogrammetric study.* Journal of Bone and Joint Surgery [Br], 1993. **75**(5): p. 681-7.
3. Maloney, W.J., et al., *Biomechanical and histologic investigation of cemented total hip arthroplasties. A study of autopsy-retrieved femurs after in vivo cycling.* Clinical Orthopaedics and Related Research, 1989(249): p. 129-40.
4. Folgado, J., et al., *Influence of femoral stem geometry, material and extent of porous coating on bone ingrowth and atrophy in cementless total hip arthroplasty: an iterative finite element model.* Computer Methods in Biomechanics and Biomedical Engineering, 2009. **12**(2): p. 135-145.
5. Pal, B., S. Gupta, and A.M.R. New, *Influence of the change in stem length on the load transfer and bone remodelling for a cemented resurfaced femur.* Journal of Biomechanics, 2010. **43**(15): p. 2908-2914.
6. Demey, G., et al., *Does a Collar Improve the Immediate Stability of Uncemented Femoral Hip Stems in Total Hip Arthroplasty? A Bilateral Comparative Cadaver Study.* The Journal of Arthroplasty, 2011. **26**(8): p. 1549-1555.
7. Whiteside, L.A., D. Amador, and K. Russell, *The Effects of the Collar on Total Hip Femoral Component Subsidence.* Clinical Orthopaedics and Related Research, 1988(231): p. 120-126.
8. Vidalain, J.P., *Twenty-year results of the cementless Corail stem.* Int Orthop, 2011. **35**(2): p. 189-94.
9. Jameson, S.S., et al., *Independent predictors of failure up to 7.5 years after 35 386 single-brand cementless total hip replacements: A retrospective cohort study using National Joint Registry data.* Bone & Joint Journal, 2013. **95-B**(6): p. 747-757.
10. Australian Orthopaedic Association National Joint Replacement Registry, *Hip and Knee Arthroplasty Annual Report 2015*. 2015, Australian National Joint Arthoplasty Register.
11. England and Wales National Joint Registry, *National Joint Registry for England and Wales 13th Annual Report*. 2016.
12. Mandell, J.A., et al., *A conical-collared intramedullary stem can improve stress transfer and limit micromotion.* Clinical Biomechanics, 2004. **19**(7): p. 695-703.
13. Whiteside, L.A. and J.C. Easley, *The Effect of Collar and Distal Stem Fixation on Micromotion of the Femoral Stem in Uncemented Total Hip-Arthroplasty.* Clinical Orthopaedics and Related Research, 1989(239): p. 145-153.
14. Callary, S.A., et al., *The 6-Year Migration Characteristics of a Hydroxyapatite-Coated Femoral Stem: A Radiostereometric Analysis Study.* The Journal of Arthroplasty, 2012. **27**(7): p. 1344-1348.e1.
15. Sudhahar, T., S. Morapudi, and K. Branes, *Evaluation of subsidence between collarless and collared corail femoral cementless total hip replacement.* J Orthopaedics, 2009. **6**(2): p. e3.
16. Meding, J.B., et al., *Comparison of collared and collarless femoral components in primary uncemented total hip arthroplasty.* The Journal of Arthroplasty, 1997. **12**(3): p. 273-280.
17. Buhler, D.W., et al., *Three-dimensional primary stability of cementless femoral stems.* Clinical Biomechanics, 1997. **12**: p. 75-86.
18. Manley, P.A., et al., *Alterations in femoral strain, micromotion, cortical geometry, cortical porosity, and bony ingrowth in uncemented collared and collarless prostheses in the dog.* The Journal of Arthroplasty, 1995. **10**(1): p. 63-73.

19. Bergmann, G., et al., *Hip contact forces and gait patterns from routine activities.* Journal of Biomechanics, 2001. **34**(7): p. 859-871.
20. Martelli, S., et al., *Extensive risk analysis of mechanical failure for an epiphyseal hip prothesis: a combined numerical–experimental approach.* Proceedings of the Institution of Mechanical Engineers, Part H: Journal of Engineering in Medicine, 2011. **225**(2): p. 126-140.
21. Viceconti, M., et al., *Large-sliding contact elements accurately predict levels of bone-implant micromotion relevant to osseointegration.* Journal of Biomechanics, 2000. **33**(12): p. 1611-1618.
22. Keaveny, T.M. and D.L. Bartel, *Effects of Porous Coating and Collar Support on Early Load- Transfer for a Cementless Hip-Prosthesis.* Journal of Biomechanics, 1993. **26**(10): p. 1205-1216.
23. Prendergast, P.J. and D. Taylor, *Stress analysis of the proximo-medial femur after total hip replacement.* J Biomed Eng, 1990. **12**: p. 379-382.
24. Kadir, M.R.A., N. Kamsah, and N. Mohlisun, *Interface Micromotion of Cementless Hip Arthroplasty: Collared vs Non-collared Stems*, in *4th Kuala Lumpur International Conference on Biomedical Engineering 2008, Vols 1 and 2*, N.A. AbuOsman, et al., Editors. 2008. p. 428-432.
25. Taylor, M., R. Bryan, and F. Galloway, *Accounting for patient variability in finite element analysis of the intact and implanted hip and knee: A review.* International Journal for Numerical Methods in Biomedical Engineering, 2013. **29**(2): p. 273-292.
26. Bryan, R., *Large scale, multi-femur computational stress analysis using a statistical shape and intensity model*, in *School of Engineering Sciences*. 2010, University of Southampton. p. 173.
27. Galloway, F., et al., *A large scale finite element study of a cementless osseointegrated tibial tray.* J Biomech, 2013. **46**(11): p. 1900-1906.
28. Bah, M.T., et al., *Inter-subject variability effects on the primary stability of a short cementless femoral stem.* Journal of biomechanics, 2015. **48**(6): p. 1032-1042.
29. Kassi, J.-P., et al., *Stair climbing is more critical than walking in pre-clinical assessment of primary stability in cementless THA in vitro.* Journal of biomechanics, 2005. **38**(5): p. 1143-1154.
30. Clement, J.G., *The Melbourne Femur Collection: the gift of tissue underpins important medical and forensic research.* VIFM Review, 2005. **3**: p. 7-11.
31. Zhang, J., et al., *An anatomical region-based statistical shape model of the human femur.* Computer Methods in Biomechanics and Biomedical Engineering: Imaging & Visualization, 2014. **2**(3): p. 176-185.
32. Morgan, E.F., H.H. Bayraktar, and T.M. Keaveny, *Trabecular bone modulus-density relationships depend on anatomic site.* J Biomech, 2003. **36**(7): p. 897-904.
33. Heller, M.O., et al., *Determination of muscle loading at the hip joint for use in pre-clinical testing.* Journal of Biomechanics, 2005. **38**(5): p. 1155-1163.
34. Morgan, E.F. and T.M. Keaveny, *Dependence of yield strain of human trabecular bone on anatomic site.* Journal of Biomechanics, 2001. **34**: p. 569-577.
35. Frost, H., *Skeletal structural adaptations to mechanical usage (SATMU): 1. Redefining Wolff's law: the bone modeling problem.* The Anatomical Record, 1990. **226**(4): p. 403-413.
36. Çehreli, M., S. Şahin, and K. Akça, *Role of mechanical environment and implant design on bone tissue differentiation: current knowledge and future contexts.* Journal of dentistry, 2004. **32**(2): p. 123-132.
37. Behrens, B.A., et al., *Numerical investigations of stress shielding in total hip prostheses.* Proceedings of the Institution of Mechanical Engineers Part H-Journal of Engineering in Medicine, 2008. **222**(H5): p. 593-600.
38. Huiskes, R., *Stress shielding and bone resorption in THA: clinical versus computer-simulation studies.* Acta Orthop Belg, 1993. **59 Suppl 1**: p. 118-29.

39. Keaveny, T.M. and D.L. Bartel, *Effects of porous coating, with and without collar support, on early relative motion for a cementless hip prosthesis.* Journal of Biomechanics, 1993. **26**(12): p. 1355-1368.
40. Dopico-Gonzalez, C., A.M. New, and M. Browne, *A computational tool for the probabilistic finite element analysis of an uncemented total hip replacement considering variability in bone-implant version angle.* Comput Methods Biomech Biomed Engin, 2010. **13**(1): p. 1-9.
41. Bah, M.T., et al., *Efficient computational method for assessing the effects of implant positioning in cementless total hip replacements.* Journal of Biomechanics, 2011. **44**: p. 1417-1422.
42. Song, Y., G. Beaupre, and S. Goodman, *Osseointegration of total hip arthroplasties: studies in humans and animals.* Journal of long-term effects of medical implants, 1998. **9**(1-2): p. 77-112.
43. Pettersen, S.H., T.S. Wik, and B. Skallerud, *Subject specific finite element analysis of stress shielding around a cementless femoral stem.* Clinical Biomechanics, 2009. **24**(2): p. 196-202.
44. Hallan, G., et al., *Medium- and long-term performance of 11 516 uncemented primary femoral stems from the Norwegian arthroplasty register.* Journal of Bone & Joint Surgery, British Volume, 2007. **89-B**(12): p. 1574-1580.
45. Martelli, S., M.E. Kersh, and M.G. Pandy, *Sensitivity of femoral strain calculations to anatomical scaling errors in musculoskeletal models of movement.* Journal of biomechanics, 2015. **48**(13): p. 3606-3615.